Effects of excess Te on the thermoelectric properties of *p*-type 25% Bi_2Te_3-75% Sb_2Te_3 single crystal and hot-pressed sinter

CHANG-WON HWANG
Thermotek, Jinchun-gun, Chungcheongbuk-do, 365-820, Korea
E-mail: y2knet@hanmail.net

DOW-BIN HYUN, HEON-PHIL HA
Metal Processing Research Center, Korea Institute of Science and Technology, Seoul 136-791, Korea
E-mail: dbhyun@kist.re.kr

TAE SUNG OH
Department of Metallurgical Engineering and Materials Science, Hong Ik University, Seoul 121-791, Korea

Effects of excess Te on the thermoelectric properties of *p*-type 25% Bi_2Te_3-75% Sb_2Te_3 single crystal and hot-pressed sinter were characterized and understood with the micro-phase diagram near the stoichiometric composition obtained by measuring the equilibrium Seebeck coefficient. Thermoelectric properties of the 25% Bi_2Te_3-75% Sb_2Te_3 single crystal were varied with the amount of excess Te, as δ-phase of the single crystal becomes less Te-deficient with adding more excess Te. However, thermoelectric properties of the hot-pressed sinter were not varied with the amount of excess Te, because the composition of δ-phase is not changed with the amount of excess Te. While a maximum figure-of-merit of 2.39×10^{-3}/K at 300 K was obtained for the 25% Bi_2Te_3-75% Sb_2Te_3 single crystal by adding 6 wt % excess Te, the hot-pressed 25% Bi_2Te_3-75% Sb_2Te_3 sinter exhibited the figure-of-merit of 2.97×10^{-3}/K regardless of the excess Te amount.

1. Introduction

The bismuth telluride-based solid solutions, widely utilized as thermoelectric materials in Peltier cooling modules, have been generally prepared by unidirectional solidification techniques such as zone melting and Bridgman methods. Despite their excellent thermoelectric properties, the unidirectionally solidified materials have poor mechanical properties due to the cleavage fracture along the basal plane of the rhombohedral structure. In addition, both the zone melting and Bridgman methods require considerable length of time to grow ingots having good thermoelectric properties. As a new processing technique, thus, hot-pressing and related methods have been applied to prepare sintered thermoelectric materials in recent years [1–8].

The figure-of-merit of thermoelectric materials depends on the materials parameter, $(m^*/m_o)^{3/2}\ \mu_o/(\kappa - \kappa_{el})$, where m^*, μ_o and κ_{el} are the effective mass, mobility of the charge carriers and electronic thermal conductivity, respectively. Therefore, various works have been performed for the bismuth telluride-based materials to find the composition which has the largest value of $(m^*/m_o)^{3/2}\mu_o/(\kappa - \kappa_{el})$. Yim *et al.* [9, 10] reported that *p*-type Bi_2Te_3-Sb_2Te_3 single crystals has the largest $(m^*/m_o)^{3/2}\mu_o/(\kappa - \kappa_{el})$ around the composition of 25% Bi_2Te_3-75% Sb_2Te_3. There are, however, to many positive holes in undoped 25% Bi_2Te_3-75% Sb_2Te_3 single crystal to optimize the figure-of-merit [11]. It has been well known that, in *p*-type Bi_2Te_3-Sb_2Te_3 alloys, holes are created by the antistructure defects generated by the occupation of Te sites with Bi and Sb atoms [12]. In the zone melting and Bridgman methods, the hole concentration is usually reduced by inhibiting the formation of antistructure defects by the addition of excess Te to the melt [10, 13, 14]. In Bi_2Te_3-Sb_2Te_3 alloy system, however, not only the phases and but also the composition of the phases are dependent upon the processing temperature as well as the nominal composition. Thus, the behavior of excess Te in the hot-pressed Bi_2Te_3-Sb_2Te_3 alloys would be different from the case for single crystals, because hot-pressing is performed at temperatures lower than those for unidirectional solidification. However, little has been reported for the effects of excess Te addition on the thermoelectric properties of the hot-pressed Bi_2Te_3-Sb_2Te_3 alloys.

For Bi_2Te_3-Sb_2Te_3 alloy system, the micro-phase diagram near the stoichiometric composition can be evaluated by measuring the equilibrium Seebeck

coefficient. Mechanical alloying is a technique in which intermetallic compounds or alloy powders are fabricated from elemental powders through a sequence of collision events inside a high-energy ball mill. It allows receiving alloy powders with size below 1 μm, and hence, sintering of the mechanically alloyed powder could reach the phase equilibrium within a relatively short time even at lower temperatures. And more, as melting process is not involved in the mechanical alloying, phase segregation can be prevented in the mechanically alloyed powders.

In the present paper, we have prepared p-type 25% Bi_2Te_3-75% Sb_2Te_3 single crystals and hot-pressed sinters with changing the amount of excess Te up to 7 wt%, and compared the effects of excess Te addition on the thermoelectric properties of the hot-pressed sinters with those for single crystals. To understand the effects of excess Te addition for the single crystals and hot-pressed sinters, we have also obtained the micro-phase diagram for 25% Bi_2Te_3-75% Sb_2Te_3 by measuring the equilibrium Seebeck coefficient.

2. Experimental

High purity (>99.99%) Bi, Sb and Te shot and granules were washed with 10% nitric acid, acetone, and distilled water to remove the surface oxide layer. To make single crystals, the appropriate amounts of Bi, Sb and Te were weighed for 25% Bi_2Te_3-75% Sb_2Te_3 composition with $0 \sim 7$ wt % excess Te and charged into carbon coated quartz tube. The quartz tube was sealed under 10^{-5} torr, and the melt was homogeneously mixed at 800°C for 5 hours using a rocking furnace. The ingot were then grown in the zone melting furnace at 800°C with growth rate of 0.1 mm/min. Rectangular specimens of $5 \times 5 \times 10\,mm^3$ were cut from the central part of the ingots along the growth direction to measure the thermoelectric properties.

To make sintered materials, the alloy powders were fabricated by the mechanical alloying. The appropriate amounts of Bi, Sb and Te were weighed for 25% Bi_2Te_3-75% Sb_2Te_3 composition with $0 \sim 7$ wt % excess Te and charged into an attrition mill under Ar atmosphere. ZrO_2 balls were used as a milling media and ball-to-powder ratio was held at 50 : 1. Mechanical alloying was performed by rotating the Al_2O_3 container at about 300 rpm for 20 hours. After the attrition milling process, X-ray diffraction (XRD) analysis was performed to confirm the complete formation of the alloy powders. A reduction treatment of powders was performed at 400°C for 24 hours in 50% H_2 + 50% Ar atmosphere to eliminate the effect of the powder-surface oxidation on the thermoelectric properties. The reduction treated alloy powders were cold pressed at 425 MPa to form $5 \times 5 \times 10\,mm^3$ compacts. Hot pressing was performed in vacuum at 550°C for 30 minutes. To obtain the equilibrium Seebeck coefficient, the cold compacts were sintered in a vacuum-sealed quartz ampoule at temperatures ranging from 150°C to 550°C until the Seebeck coefficient equilibrated. At the higher temperature of 500°C, the Seebeck coefficient of the mechanically alloyed sinters reached equilibrium within 1 hour, while at the lower temperature of 150°C took it at least 7 days.

Differential Thermal Analysis (DTA) was performed in Ar atmosphere at a scan rate of 5°C/min for the as-mixed and mechanically alloyed powders. The Seebeck coefficient (α) was measured by applying a temperature difference of 10°C at both ends of the specimen. The electrical resistivity (ρ) and the figure-of-merit (Z) were measured using the Harman method [15] at 10^{-5} torr to minimize the thermal conduction through convection. The thermal conductivity (κ) was determined using the relationship $\kappa = \alpha^2/Z\rho$.

3. Results and discussion

3.1. Equilibrium Seebeck coefficient near the stoichiometric composition

XRD patterns of the as-mixed and mechanically alloyed powders, shown in Fig. 1, clearly revealed the formation of 25% Bi_2Te_3-75% Sb_2Te_3 alloy from elemental Bi, Sb and Te powders by mechanical alloying at room temperature. DTA curves of the as-mixed and mechanically alloyed 25% Bi_2Te_3-75% Sb_2Te_3 powders are shown in Fig. 2. For the as-mixed powder, endothermic peaks were observed at 272°C, 423°C and 617°C due to the melting of Bi, Te-rich Bi-Sb-Te eutectic, and 25% Bi_2Te_3-75% Sb_2Te_3, respectively. Exothermic peak at 531°C was due to the formation reaction of 25% Bi_2Te_3-75% Sb_2Te_3 solid solution. Such peaks except one at 617°C disappeared in DTA for mechanically alloyed powder, which indicated the formation of 25% Bi_2Te_3-75% Sb_2Te_3 by mechanical alloying. Endothermic peak at 417°C was due to the melting of Te-rich second phase [16, 17]. On the basis of DTA results, thus, it could be known that the equilibrium microstructural phase of the stoichiometric 25% Bi_2Te_3-75% Sb_2Te_3 composition is (δ + Te) below 417°C, and (liq. + δ) between 417°C and 617°C.

The equilibrium Seebeck coefficient of the sintered 25% Bi_2Te_3-75% Sb_2Te_3 are shown in Fig. 3 as a function of sintering temperature. The Seebeck coefficient of cold pressed 25% Bi_2Te_3-75% Sb_2Te_3 was about 163 μV/K. After sintering, however, the equilibrium

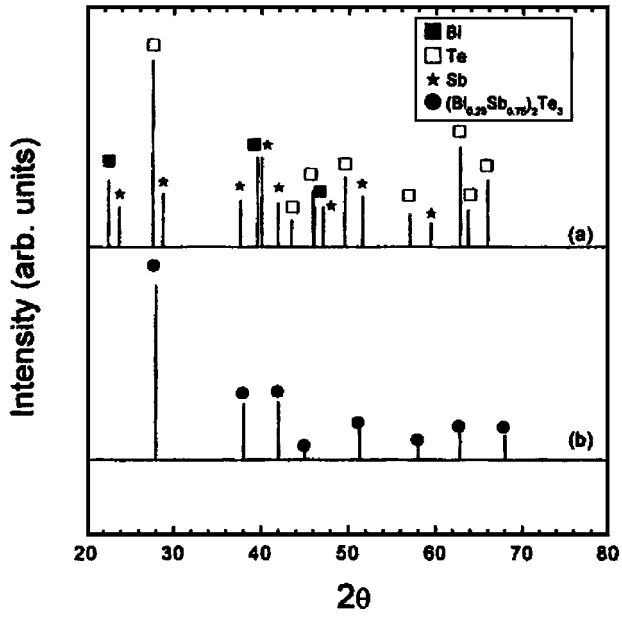

Figure 1 XRD patterns of (a) as-mixed and (b) mechanically alloyed powders for 25% Bi_2Te_3-75% Sb_2Te_3 composition.

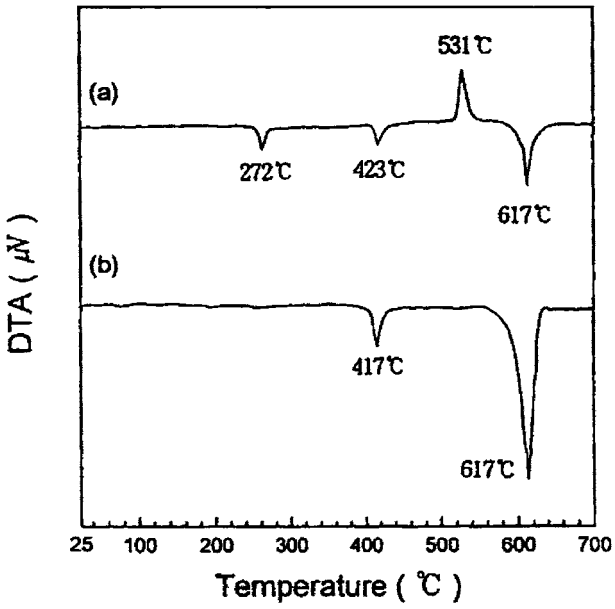

Figure 2 DTA curves of (a) as-mixed and (b) mechanically alloyed powders for 25% Bi_2Te_3-75% Sb_2Te_3 composition.

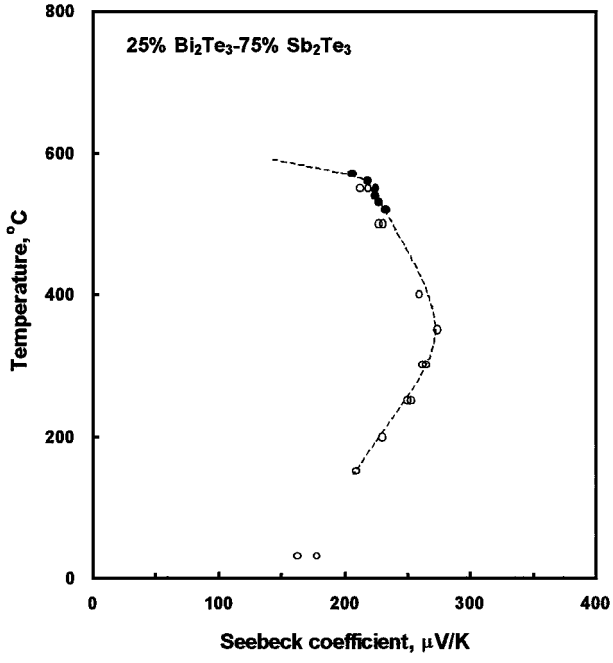

Figure 3 Equilibrium Seebeck coefficient of 25% Bi_2Te_3-75% Sb_2Te_3 as a function of the sintering temperature.

Seebeck coefficient was increased with temperature up to 274 μV/K at 350°C and then decreased with further increase of the sintering temperature. For the 25% Bi_2Te_3-75% Sb_2Te_3 single crystals, Scherrer *et al.* [18, 19] studied the equilibrium Seebeck coefficient at the solidus line between 520°C and 570°C using the travelling heater method (THM). The data from Scherrer *et al.* are also shown in Fig. 3 (solid circles) for comparison. Coincidence of the Seebeck coefficient of the sintered specimens with those of the single crystals revealed that the equilibrium phases could be obtained by sintering the mechanically alloyed specimens until the Seebeck coefficient was equilibrated.

Generally, p-type Bi_2Te_3-Sb_2Te_3 single crystals are non-stoichiometric and deviated from the stoichiometry toward bismuth and antimony because Te is more volatile than Bi and Sb [20]. Antistructure defects of Bi_{Te} and Sb_{Te} are created by the occupation of the vacant Te site with Bi and Sb, and holes are generated by [20, 21]

$$\begin{aligned} Bi_2Te_3 &= 2Bi'_{Te} + V^x_{Te} + 2V^x_{Bi} + (3/2)Te_{2(g)} + 2h^\bullet \\ Sb_2Te_3 &= 2Sb'_{Te} + V^x_{Te} + 2V^x_{Sb} + (3/2)Te_{2(g)} + 2h^\bullet \end{aligned} \quad (1)$$

Thus, the hole concentration (p) of p-type Bi_2Te_3-Sb_2Te_3 alloys is determined by the antistructure defect concentration which is dependent upon the degree of Te-deficiency from the stoichiometric composition. Assuming Boltzmann distribution, the Seebeck coefficient of p-type thermoelectric materials is related with the hole concentration as follows;

$$\alpha = \frac{k_B}{e}\left[s + \frac{5}{2} + \ln\frac{2(2\pi m^* k_B T)^{3/2}}{ph^3}\right] \quad (2)$$

where k_B is the Boltzmann constant, s the scattering parameter, h the Plank's constant and m^* the effective mass. From the equilibrium Seebeck coefficient in Fig. 3, thus, the degree of Te-deficiency from the stoichiometric composition, i.e. a micro-phase diagram near the stoichiometric composition of 25% Bi_2Te_3-75% Sb_2Te_3 solid solution was evaluated as illustrated in Fig. 4. The solidus line is shifted from the stoichiometry toward bismuth and antimony in the (liq. + δ) region.

3.2. Effects of excess Te on thermoelectric properties of single crystals

25% Bi_2Te_3-75% Sb_2Te_3 single crystals with 0 ~ 7 wt % excess Te were grown by the zone melting method, and the Seebeck coefficient was measured at

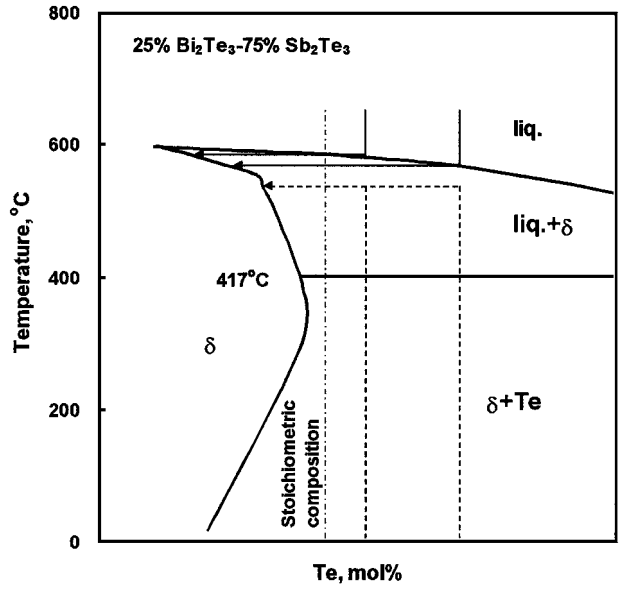

Figure 4 Micro-phase diagram near the stoichiometric composition of 25% Bi_2Te_3-75% Sb_2Te_3.

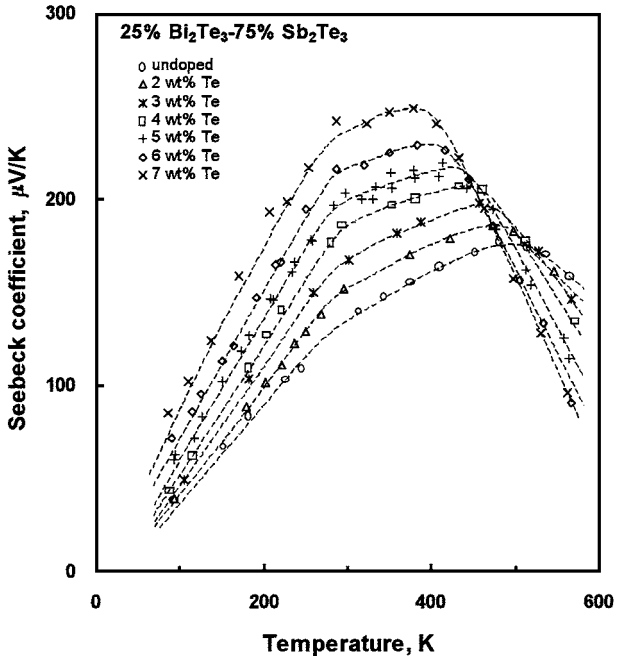

Figure 5 Temperature dependence of the Seebeck coefficient for the excess Te-doped 25% Bi_2Te_3-75% Sb_2Te_3 single crystals.

temperatures ranging from 77 K $\sim$ 600 K. Temperature dependence of the Seebeck coefficient is shown in Fig. 5. Regardless the amount of excess Te, the Seebeck coefficient initially increased with increasing temperature and then decreased after reaching a maximum value. Such increase of the Seebeck coefficient at lower temperature range is due to the decrease of the reduced Fermi energy at the carrier saturation region and the decrease of the Seebeck coefficient at higher temperatures is associated to the onset of the mixed conduction [22]. As the number of electrons thermally excited from the valence band to the conduction band increases substantially at high temperature region, the mixed conduction occurs by holes in the valence band and electrons in the conduction band, and the Seebeck coefficient can be expressed by

$$\alpha = \frac{\alpha_h \cdot \sigma_h - |\alpha_e \cdot \sigma_e|}{\sigma_h + \sigma_e} \quad (3)$$

where, α_h and α_e are the Seebeck coefficients by holes and electrons, respectively, and σ_h and σ_e are the electrical conductivity by holes and electrons, respectively. Thus, the decrease of the Seebeck coefficient with increasing temperature is due to the increase of the electron contribution.

As shown in Fig. 5, the maximum value of the Seebeck coefficient increased and the temperature at which the Seebeck coefficient has its maximum shifted to lower temperature with increasing the amount of excess Te. From the micro-phase diagram in Fig. 4, one could expect that the chemical composition of δ-phase for the unidirectionally grown ingot becomes less Te-deficient with adding more Te in the melt. Thus, the Seebeck coefficient of the 25% Bi_2Te_3-75% Sb_2Te_3 single crystal increased with adding more excess Te due to the lower concentration of antistructure defects, i.e. lower hole concentration.

The temperature dependence of the electrical resistivity for the 25% Bi_2Te_3-75% Sb_2Te_3 single crystals with 0 $\sim$ 7 wt % excess Te is shown in Fig. 6. Increase of the electrical resistivity at lower temperature region is mainly due to the decrease of the carrier mobility, and the decrease of the electrical resistivity after reaching a maximum is attributed to the onset of the mixed conduction [23]. The electrical resistivity increased with the addition of more excess Te, which was due to the lesser carrier concentration. The thermal conductivity and the figure-of-merit ($Z = \alpha^2/\rho k$) of the 25% Bi_2Te_3-75% Sb_2Te_3 single crystals with 0 $\sim$ 7 wt % excess Te are shown in Figs 7 and 8, respectively. With increasing

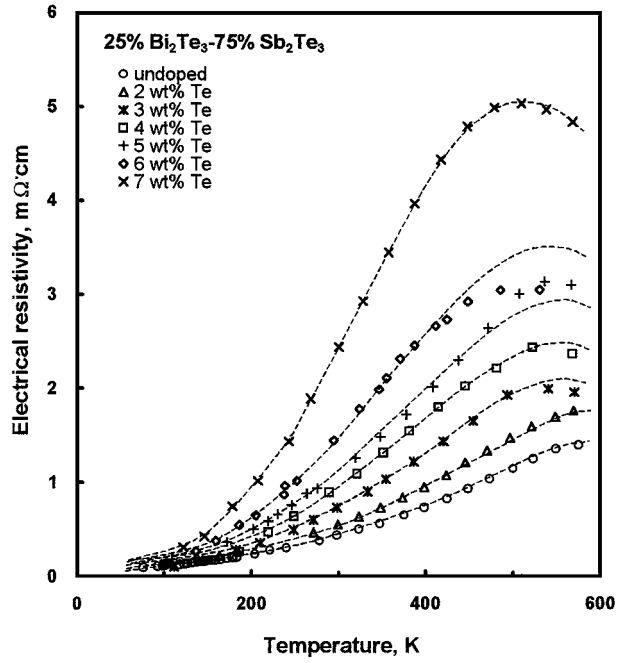

Figure 6 Temperature dependence of the electrical resistivity for the excess Te-doped 25% Bi_2Te_3-75% Sb_2Te_3 single crystals.

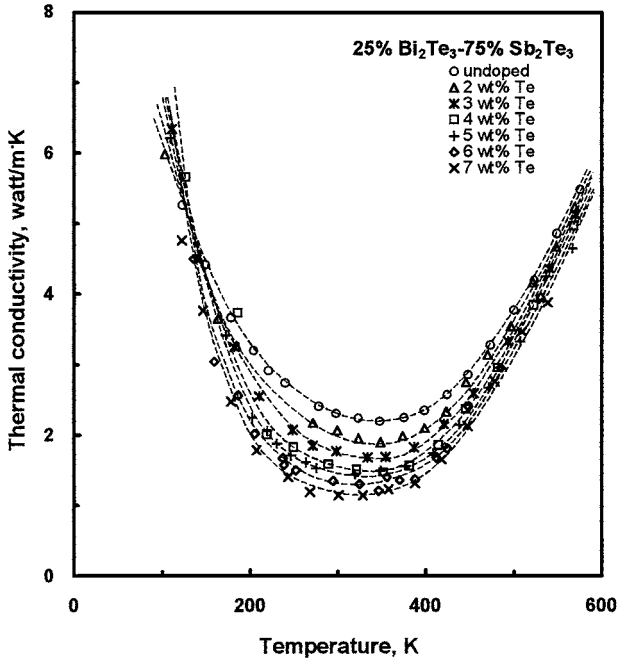

Figure 7 Temperature dependence of the thermal conductivity for the excess Te-doped 25% Bi_2Te_3-75% Sb_2Te_3 single crystals.

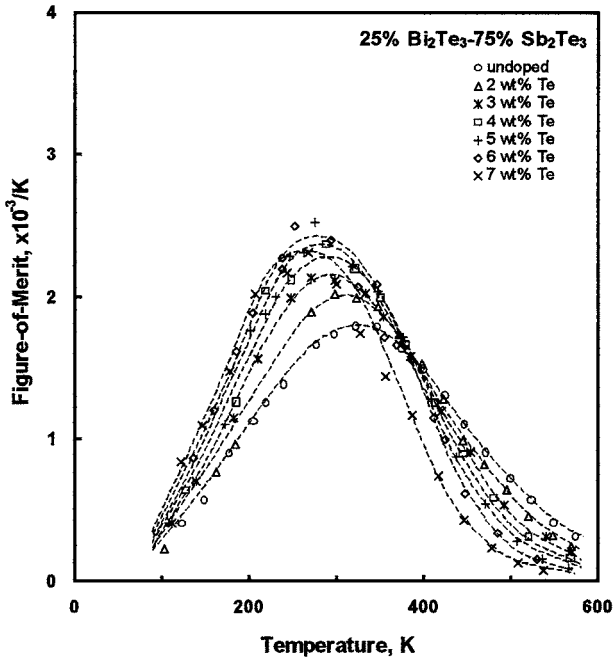

Figure 8 Temperature dependence of the figure-of-merit for the excess Te-doped 25% Bi_2Te_3-75% Sb_2Te_3 single crystals.

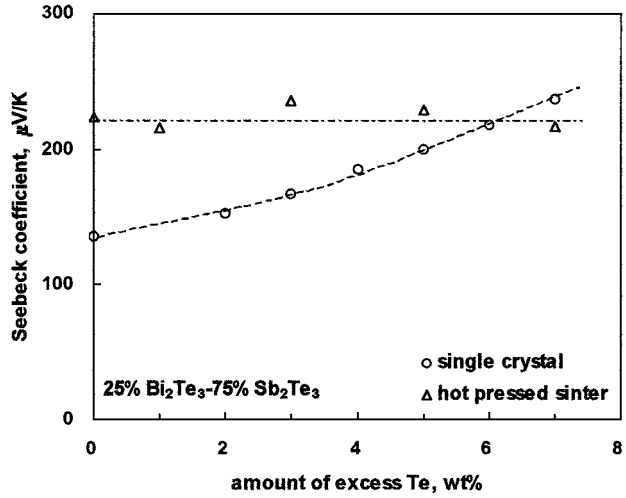

Figure 9 Seebeck coefficient of the excess Te-doped 25% Bi_2Te_3-75% Sb_2Te_3 hot-pressed sinters and single crystals at room temperature.

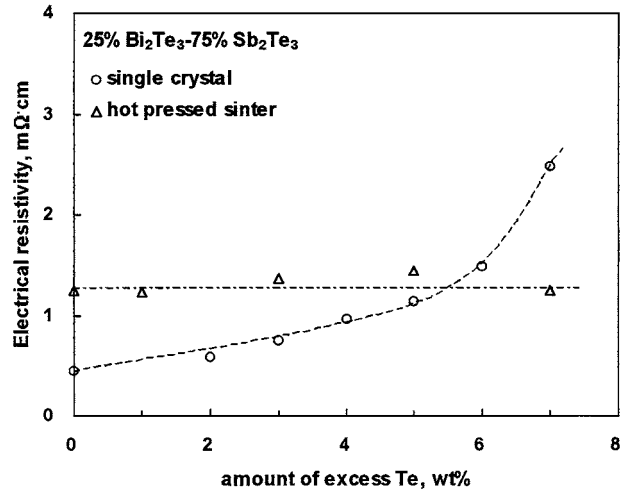

Figure 10 Electrical resistivity of the excess Te-doped 25% Bi_2Te_3-75% Sb_2Te_3 hot-pressed sinters and single crystals at room temperature.

the temperature, the thermal conductivity initially decreased and then increased after reaching its minimum at about 300 K. At the same temperature, the thermal conductivity decreased with increasing the amount of excess Te. The figure-of-merit increased initially with increasing temperature, showed the maximum at about 300 K, and then decreased with further increase of the temperature. With increasing the amount of excess Te, the temperature at which the figure-of-merit has a maximum shifted to lower temperature due to the decrease of the hole concentration [9]. Since the Seebeck coefficient and the electrical resistivity increased simultaneously with the addition of excess Te, the optimum amount of excess Te exists to improve the figure-of-merit of 25% Bi_2Te_3-75% Sb_2Te_3 single crystals. For the $0 \sim 7$ wt % excess Te doped 25% Bi_2Te_3-75% Sb_2Te_3 single crystals, a maximum figure-of-merit of 2.39×10^{-3}/K at 300 K was obtained by adding 6 wt % excess Te.

3.3. Effects of excess Te on thermoelectric properties of hot-pressed sinters

To examine the effect of excess Te doping on the thermoelectric properties of the hot-pressed 25% Bi_2Te_3-75% Sb_2Te_3 sinters, mechanically alloyed powders doped with excess Te up to 7 wt % were hot-pressed in a vacuum at 550°C for 30 minutes. The Seebeck coefficient and the electrical resistivity at room temperature for the hot-pressed 25% Bi_2Te_3-75% Sb_2Te_3 sinters are shown as a function of excess Te in Figs 9 and 10, respectively. Data from the single crystals are also plotted for comparison. While the Seebeck coefficient and the electrical resistivity of the single crystals increased with the amount of excess Te due to the reduction of the carrier concentration, those of the hot-pressed specimens were almost unchanged regardless the amount of excess Te. The Seebeck coefficient of the hot-pressed specimens was about 225 μV/K, which was in good agreement with the equilibrium Seebeck coefficient at 550°C shown in Fig. 3. When the 25% Bi_2Te_3-75% Sb_2Te_3 powders with different amount of excess Te are hot-pressed at 550°C in the (liq. + δ) region, the ratio of solid phase δ and liquid phase is changed according to the level rule. However, the composition of the δ-phase is the same regardless the amount of excess Te, as shown by the dotted line in Fig. 4. Even with changing the amount of excess Te up to 7 wt %, thus, the hot-pressed specimens were composed of δ matrix of the same chemical composition with small amount of Te-rich second phase that was solidified from the liquid phase. The amount of Te-rich second phase would increase with the addition of more excess Te. However, the Seebeck coefficient and electrical resistivity of the excess Te-doped 25% Bi_2Te_3-75% Sb_2Te_3 sinters were little affected by the amount of Te-rich second phase [24].

The thermal conductivity at room temperature for the hot-pressed sinters and single crystals are shown in Fig. 11 as a function of excess Te. While the thermal

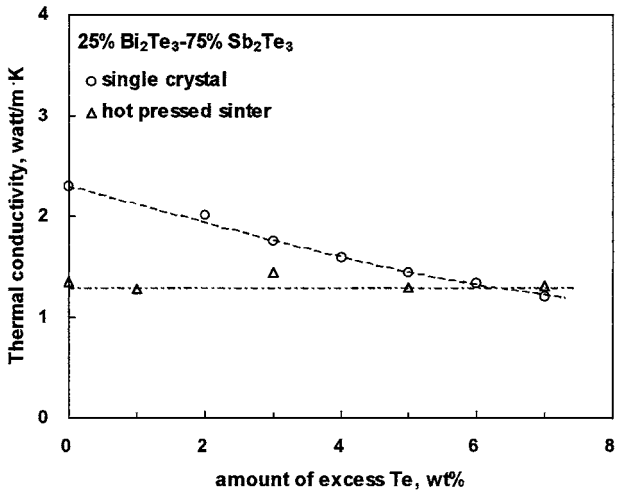

Figure 11 Thermal conductivity of the excess Te-doped 25% Bi_2Te_3-75% Sb_2Te_3 hot-pressed sinters and single crystals at room temperature.

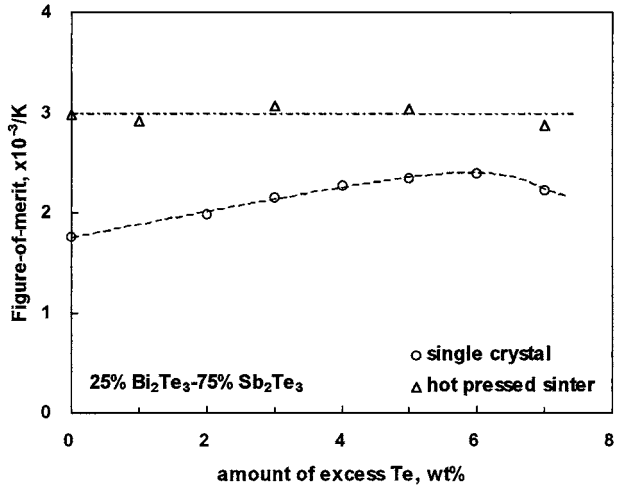

Figure 12 Figure-of-merit of the excess Te-doped 25% Bi_2Te_3-75% Sb_2Te_3 hot-pressed sinters and single crystals at room temperature.

conductivity of the single crystals was reduced with the addition of more excess Te mainly due to the decrease of the electronic thermal conductivity, $\kappa_{el} = L\sigma T$ (L : Lorentz number, σ : electrical conductivity), the thermal conductivity of the hot-pressed specimens was the same regardless of the amount of excess Te. The figure-of-merit of the hot-pressed sinters and single crystals at room temperature is shown in Fig. 12. The figure-of-merit of the single crystals was improved with increasing the amount of excess Te and showed a maximum value of 2.39×10^{-3}/K with adding 6 wt % excess Te. Contrary to the single crystals, the hot-pressed 25% Bi_2Te_3-75% Sb_2Te_3 sinters exhibited the figure-of-merit of 2.97×10^{-3}/K which was little changed with the variation of the excess Te amount up to 7 wt %. From our results, it can be concluded that the carrier concentration and, thus, the thermoelectric properties of the p-type Bi_2Te_3-Sb_2Te_3 single crystals are controlled by the addition of the excess Te. However, the carrier concentration and thermoelectric properties of the hot-pressed p-type Bi_2Te_3-Sb_2Te_3 sinters are not controlled with the variation of the excess Te amount, because the chemical composition of δ matrix phase is not changed. Rather, thermoelectric properties of the hot-pressed p-type Bi_2Te_3-Sb_2Te_3 sinters can be controlled by changing the hot-pressing or sintering temperature to vary the Te-deficiency of δ matrix phase.

4. Conclusions

The micro-phase diagram near the stoichiometric composition of 25% Bi_2Te_3-75% Sb_2Te_3 solid solution was obtained by measuring the equilibrium Seebeck coefficient. The solidus line is shifted from the stoichiometry toward bismuth and antimony in the (liq. + δ) region. The carrier concentration and, thus, the thermoelectric properties of the p-type 25% Bi_2Te_3-75% Sb_2Te_3 single crystals could be controlled by the addition of the excess Te. From the micro-phase diagram, it could be known that δ-phase of the unidirectionally grown ingot becomes less Te-deficient with adding more excess Te, resulting in the decrease of the hole concentration. A maximum figure-of-merit of 2.39×10^{-3}/K at 300 K was obtained for the 25% Bi_2Te_3-75% Sb_2Te_3 single crystals by adding 6 wt % excess Te. However, the carrier concentration and thermoelectric properties of the hot-pressed 25% Bi_2Te_3-75% Sb_2Te_3 sinters were not controlled with the variation of the excess Te amount, because the composition of δ matrix phase was not changed with the amount of excess Te. The hot-pressed p-type 25% Bi_2Te_3-75% Sb_2Te_3 sinters exhibited the figure-of-merit of 2.97×10^{-3}/K regardless of the excess Te amount. On the basis of the micro-phase diagram, it is suggested that the thermoelectric properties of the hot-pressed p-type Bi_2Te_3-Sb_2Te_3 sinters can be controlled by changing the hot-pressing or sintering temperature to vary the Te-deficiency of δ matrix phase.

References

1. W. R. GEORGE, R. SHARPLES and J. E. THOMPSON, *Proc. Phys. Soc. LXXIV* **6** (1959) 769.
2. G. V. KOKOSH and S. S. SINANI, *Soviet Phys. Sol. State* **2** (1961) 1021.
3. F. FUKUDA, A. ONODERA and H. HAGA, in Proceedings of the 12th International Conference on Thermoelectrics, Yokohama, Japan, November 1993, edited by K. Matsuura (1993) p. 24.
4. K. NAKAMURA, K. MORIKAWA, H. OWADA, K. MIURA, K. OGAWA and I. A. NISHIDA, in Proceedings of the 12th International Conference on Thermoelectrics, Yokohama, Japan, November 1993, edited by K. Matsuura (1993), p. 110.
5. A. YANAGITANI, S. NISHIKAWA, Y. KAWAI, S. HATASHIMOTO, N. ITOH and T. KATAOKA, in Proceedings of the 12th International Conference on Thermoelectrics, Yokohama, Japan, November 1993, edited by K. Matsuura (1993) p. 281.
6. K. HASEZAKI, M. NISHIMURA, M. UMATA, H. TSUKUDA and M. ARAOKA, in Proceedings of the 12th International Conference on Thermoelectrics, Yokohama, Japan, November 1993, edited by K. Matsuura (1993) p. 307.
7. B. Y. JUNG, S. E. NAM, D.-B. HYUN, J.-D. SHIM and T. S. OH, *J. Korean Inst. Metal & Mater.* **35** (1997) 153.
8. H. J. KIM, J. S. CHOI, D.-B. HYUN and T. S. OH, *ibid.* **35** (1997) 223.
9. W. M. YIM, E. V. FITZKE and F. D. ROSI, *J. Mater. Sci.* **1** (1966) 52.
10. W. M. YIM and F. D. ROSI, *Solid State Electronics* **15** (1972) 1121.
11. H.-W. JEON, H.-P. HA, D.-B. HYUN and J.-D. SHIM, *J. Phys. Chem. Solids* **52** (1991) 579.
12. G. R. MILLER and C.-Y. LI, *ibid.* **26** (1965) 173.

13. R. B. HORST and L. R. WILLIAMS, in Proceedings of the 4th International Conference on Thermoelectric Energy Conversion, Arlington, Texas, March 1982, edited by K. R. Rao (1982) p. 119.
14. A. I. ANUKHIN and O. B. SOKOLOV, in Proceedings of the 11th International Conference on Thermoelectric Energy Conversion, Arlington, Texas, October 1992, edited by K. R. Rao (1992) p. 307.
15. T. C. HARMAN, J. H. CAHN and M. J. LOGAN, *J. Appl. Phys*. **30** (1959) 1351.
16. N. KH. ABRIKOSOV and L. V. PORETSKAYA, *Izv. AN SSSR, Neorganich. Materialy* **1** (1965) 503.
17. N. KH. ABRIKOSOV, V. F. BANKINA, L. V. PORETSKAYA, L. E. SHELIMOVA and E. V. SKUDNOVA, in "Semiconducting II-VI, IV-VI, and V-VI Compounds" (Plenum Press, New York, 1969) p. 164.
18. T. CAILLAT, M. CARLE, P. PIERRAR, H. SCHERRER and S. SCHERRER, *J. Phys. Chem. Solids* **53** (1992) 1121.
19. H. SCHERRER and S. SCHERRER, in Proceedings of the 12th International Conference on Thermoelectrics, Yokohama, Japan, November 1993, edited by K. Matsuura (1993) p. 90.
20. J. HORAK, K. CERMAK and L. KOUDELKA, *J. Phys. Chem. Solids* **47** (1986) 805.
21. B. A. COOK, B. J. BEAUDRY, J. L. HARRINGA and W. J. BARNETT, in Proceedings of the 24th Intersociety Energy Conversion Engineering Conference (1989) p. 693.
22. D.-B. HYUN, J.-S. HWANG, B.-C. TOU, T. S. OH and C.-W. HWANG, *J. Mater. Sci*. **33** (1998) 5595.
23. D.-B. HYUN, H.-P. HA, J.-D. SHIM, J.-S. HWANG and T. S. OH, *J. Korean Inst. Metal & Mater*. **37** (1999) 980.
24. D. M. GEL'FGAT and Z. M. DASHEVSKII, *Inorg. Mater*. **19** (1984) 1172.

Received 18 February 2000
and accepted 6 February 2001